



Analyses of Pulse-Shaped Signals based on Two-Dimensional Probability Distributions

Tomoya Fukami^{*(1)}, Hirobumi Saito⁽²⁾, and Akira Hirose⁽¹⁾

(1) The University of Tokyo, Tokyo, Japan; e-mail: fukami@eis.t.u-tokyo.ac.jp; ahirose@ee.t.u-tokyo.ac.jp

(2) Waseda University, Tokyo, Japan; e-mail: saito.hirobumi@aoni.waseda.jp

Abstract

This paper presents the analyses of the pulse-shaped signals based on the probability distribution on the in-phase and quadrature-phase (I/Q) complex plane. The two-dimensional distribution is obtained quickly by the recursive probability mass function method. In this paper, we analyze the 8PSK, 16APSK, and 32APSK signals defined in the DVB-S2 standard. The results indicate that the peak amplitude of each I/Q signal for 8PSK and 32APSK can be reduced by rotating the placement of the symbols. The two-dimensional distribution-based analysis provides valuable insights that cannot be obtained with existing instantaneous power distribution-based analyses.

1 Introduction

Finite impulse response (FIR) filters are used for pulse shaping in various radiocommunication systems. The probability distribution of the pulse-shaped signals helps us to understand the characteristics of the signals and optimize the systems. Many methods have been proposed to obtain the complementary cumulative distribution function (CCDF) of instantaneous power and the peak-to-average power ratio (PAPR) [1, 2, 3, 4, 5].

In particular, the method in Ref. [4] is distinguished because it provides the exact distributions of instantaneous power. The exact method is described as being applicable to arbitrary constellations, and the characteristic functions for phase-shift keying (PSK) and quadrature amplitude modulation (QAM) are given as examples. However, in contrast to QAM, where the symbols are placed in a regular grid pattern, amplitude and phase-shift keying (APSK), which is often used in satellite communications and broadcasting [6, 7, 8], has more freedom in symbol placement. It is not easy to derive the characteristic function of APSK.

Recently, we proposed the recursive probability mass function method (our method) [9] to calculate probability distributions of pulse-shaped signals. Our method is free from the derivation of the characteristic function required in the exact method. This fact results in its easy application to arbitrary constellations just like brute-force and Monte Carlo approaches. Furthermore, the distribution on the in-phase and quadrature-phase (I/Q) complex plane is also obtained in addition to the CCDF of instantaneous power.

In this paper, we analyze the 8PSK, 16APSK, and 32APSK signals defined in the DVB-S2 standard [6] using the recursive probability mass function method. We show that the two-dimensional distribution provides valuable insights that cannot be obtained with CCDF or PAPR.

2 Signal Model and Probability Distribution

Let $\mathcal{Z} = \{Z_0, Z_1, \dots, Z_{Q-1}\}$ denote a set of complex modulation symbols, where Q is the modulation order, e.g., $Q = 4$ for QPSK. The symbol sequence $x[k]$ is expressed as

$$x[k] \in \mathcal{Z}, \quad \forall k \in \mathbb{Z}, \quad (1)$$

where k is a discrete-time index. The pulse-shaped signal $y(t)$ is expressed as

$$y(t) = \sum_{k=-\infty}^{\infty} x[k]h(t-kT), \quad \forall t \in \mathbb{R}, \quad (2)$$

where t is a continuous time, $h(t)$ is the impulse response of the pulse-shaping filter, and T is the symbol interval.

In our approach [9], we introduce signal quantization to calculate distributions efficiently. The quantized pulse-shaped signal is expressed as

$$y'(t) = \sum_{k=-\infty}^{\infty} \frac{1}{A} \lfloor Ax[k]h(t-kT) \rfloor, \quad (3)$$

where $\lfloor \cdot \rfloor$ represents rounding to the nearest Gaussian integer and $A (> 0)$ is an amplitude-scaling parameter. As the value of A increases, the quantization resolution is increased, and the quantization error is reduced.

Let $f_{y'}(z)$ denote the probability mass function of the pulse-shaped signal y' , expressed as

$$f_{y'}(z) = \Pr(y'(t) = z), \quad \forall z \in \mathbb{C}, \forall t \in \mathbb{R}. \quad (4)$$

The recursive probability mass function method calculates (4) efficiently by dynamic programming. The accuracy of the distribution is controlled by the amplitude-scaling parameter A .

The CCDF of instantaneous power p is obtained from $f_{y'}(z)$ by summing the probabilities outside the circle of radius \sqrt{p} centered at the origin ($z = 0$) as

$$\Gamma(p) = \sum_{|z|^2 \geq p} f_{y'}(z). \quad (5)$$

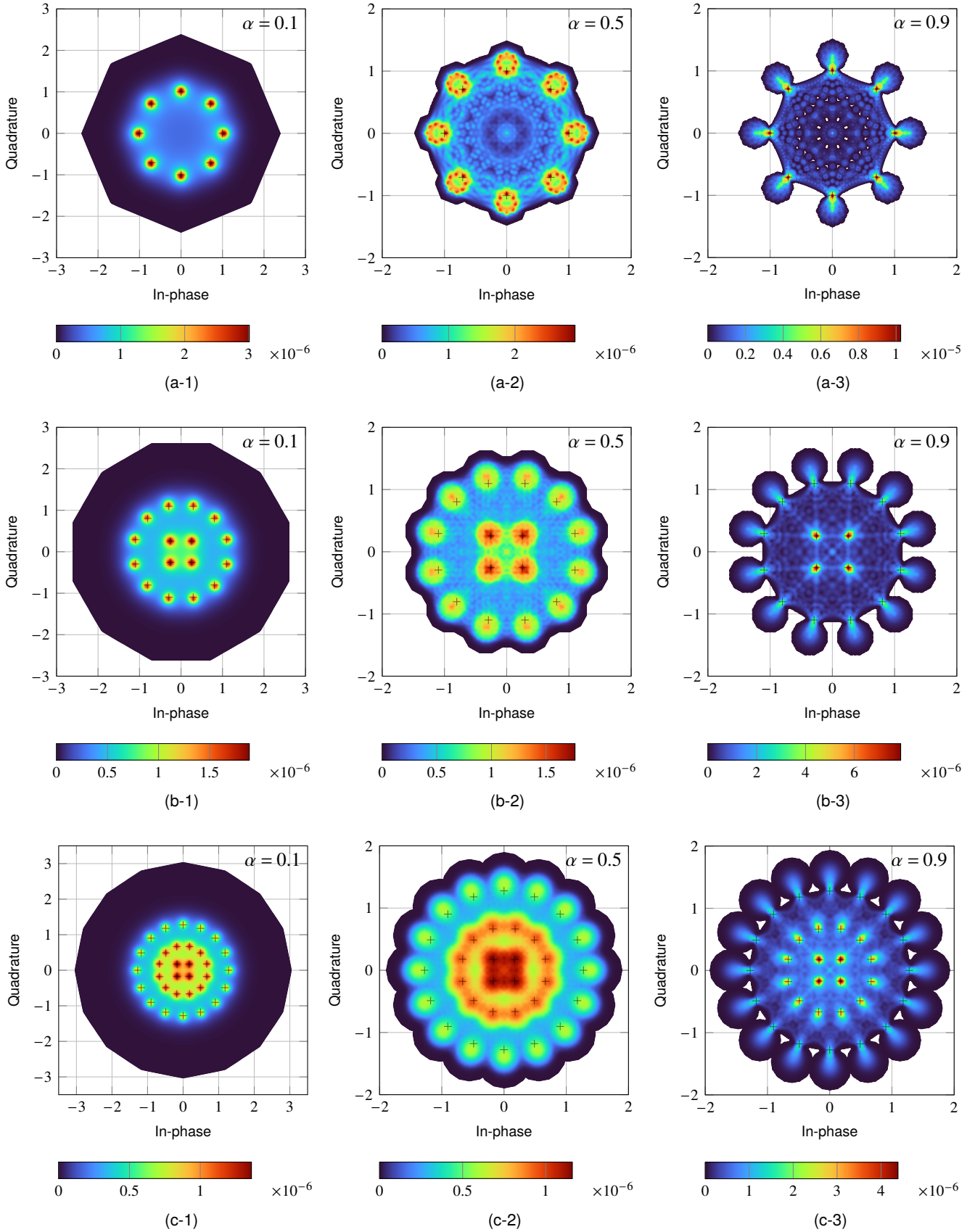


Figure 1. Two-dimensional distributions $f_y(z)$ on the complex plane for (a-★) 8PSK, (b-★) 16APSK, and (c-★) 32APSK. The roll-off factor α is 0.1 for (★-1), 0.5 for (★-2), and 0.9 (★-3). The black crosses show the locations of the symbols, and the white area means that the probability is zero. The color scale is adjusted for each figure.

3 Analysis Results

In this section, we show the analysis results. Unless otherwise mentioned, it is performed under the following conditions. Root raised-cosine (RRC) and full raised-cosine (FRC) filters, shown in Ref. [10], are used as the pulse-shaping filters. The roll-off factor of the RRC filter is denoted by α . The oversampling rate is 32 and the order of the pulse-shaping filter is 36×32 . In the DVB-S2 standard [6], the radius ratios of 16APSK and 32APSK depend on the code rate r of the forward error correction code. In this paper, 16APSK ($r = 2/3$) and 32APSK ($r = 3/4$) are analyzed.

3.1 Two-dimensional distributions

Figure 1 shows the obtained two-dimensional distributions for (a-★) 8PSK, (b-★) 16APSK, and (c-★) 32APSK. The roll-off factor α is 0.1 for (★-1), 0.5 for (★-2), and 0.9 (★-3). The color represents the probability of occurrence of each I/Q cell. The black crosses show the locations of the symbols, and the white area means that the probability is zero. The color scale is adjusted for each figure. The amplitude-scaling parameter A in (3) is 500.

Figure 1 (a-1) shows that the 8PSK signal with RRC filter ($\alpha = 0.1$) has high-probability regions around the eight symbols. The distribution shows an octagonal shape on the complex plane. The amplitudes of the peak power points are larger than twice the symbol points. Figure 1 (a-2) and (a-3) show that the shape of the probability distributions is no longer octagonal. Interestingly, the PAPR for $\alpha = 0.5$ is the smallest in (a-★). In other words, the relationship between PAPR and α is nonlinear.

Furthermore, we find that the peak amplitude of each I/Q signal is decreased by rotating the symbol position by $\frac{45}{2}$ degrees. This is an important finding when I/Q signals are processed independently. Since the average amplitude in limited resolution can be increased by the rotation, the signal-to-noise ratio is improved in digital signal processing and digital-to-analog (D/A) converters.

Figure 1 (b-1) shows that the distribution of the 16APSK signal with RRC filter ($\alpha = 0.1$) is a dodecagon shape on the complex plane. In contrast to the 8PSK, rotating the symbol position does not reduce the peak amplitude of each I/Q signal. In other words, 16APSK is already the optimal symbol placement.

From Fig. 1 (c-★), we find that the peak amplitude of each I/Q signal is decreased by rotating the symbol position by $\frac{45}{4}$ degrees. Comparing (a-1) and (c-1), the improvement is smaller than that in the case of 8PSK.

From Fig. 1 (★-3), the distributions of the signals with RRC filter ($\alpha = 0.9$) are shaped like a coronavirus. The spike protein-like regions seem to grow as α increases. Although

the growth mechanism cannot be directly clarified from the two-dimensional distributions, we can see how PAPR becomes higher when α is increased.

The two-dimensional distribution cannot be obtained by any other methods of calculating instantaneous power distributions. The probability of saturation in digital signal processing and D/A converters is obtained by summing the probabilities outside the rectangle centered at the origin ($z = 0$). The CCDFs of instantaneous power obtained by (5) are shown in the next section.

3.2 CCDFs of instantaneous power

Figure 2 compares the CCDFs of the instantaneous power for the same nine types of signals as in Fig. 1. The solid lines are obtained by our method with $A = 2,000$, and the dots are obtained by the corresponding Monte Carlo simulations with 10^6 symbols. Since the oversampling rate is 32, the number of samples in Monte Carlo simulations is 32×10^6 .

The distributions obtained by our method match well with the corresponding Monte Carlo simulations in the high-probability region. Differences in around $\Gamma(p) = 10^{-8}$ region are due to the insufficient number of samples in the Monte Carlo simulations. The PAPR of the signals with $\alpha = 0.1$ is particularly high. While the PAPR of the 32APSK signal ($\alpha = 0.1$) obtained by Monte Carlo simulation is about 8 dB, the PAPR obtained by our method is about 9.6 dB. Although the probability of peak power occurrence is low, it is important to know that such high-power signals can occur. Unanticipated high-power signals can cause system failures, adjacent channel interference, and electromagnetic compatibility issues.

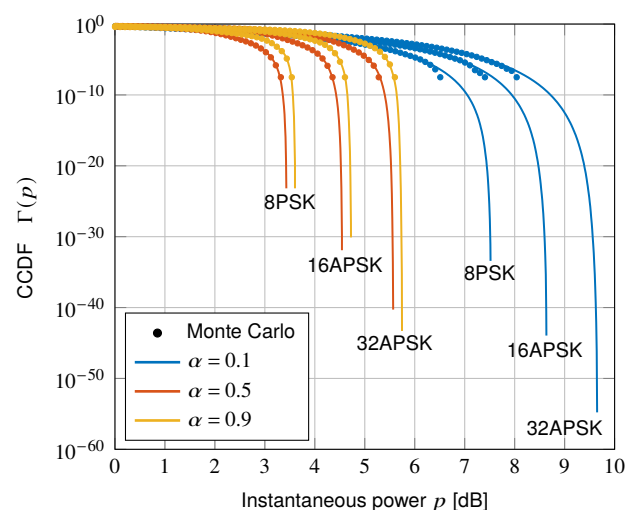


Figure 2. Comparison of CCDFs obtained with our method and Monte Carlo simulations. The solid lines are obtained by our method with $A = 2,000$, and the dots are obtained by the corresponding Monte Carlo simulations with 10^6 symbols.

3.3 Computation time

Finally, we evaluate the computation time. All calculations were performed on Intel® Xeon® Platinum 8368 processor with 512 GB memory and NVIDIA® A100 graphics processing unit (GPU) with 40 GB memory. Since most calculations are performed on the GPU, the performance of the GPU determines the computation time.

Figure 3 shows the obtained probability of peak power occurrence with respect to computation time. The amplitude-scaling parameter A is varied in our method, and the number of samples is varied in the Monte Carlo simulations. Since the result of the Monte Carlo simulation is independent of the signal format, the result for 64QAM with FRC filter ($\alpha = 0.1$) is plotted as an example. Our method obtains probabilities consistent with or close to the theoretical values in less than 10 seconds of computation time. On the other hand, it is hard to obtain probabilities consistent with theoretical values by Monte Carlo simulation.

4 Conclusion

We have analyzed the 8PSK, 16APSK, and 32APSK signals defined in the DVB-S2 standard. By observing the two-dimensional distributions, we found that 8PSK should be rotated $\frac{45}{2}$ degrees and 32APSK should be rotated $\frac{45}{4}$ degrees in terms of the dynamic range of each I/Q signal. The CCDF of instantaneous power or PAPR-based analysis cannot find those facts. The two-dimensional distributions of pulse-shaped signals are efficiently obtained by the recursive probability mass function method [9].

Acknowledgements

This work was partly supported by JSPS KAKENHI Grant Number JP16J07353 (TF) and partly achieved through the use of SQUID at the Cybermedia Center, Osaka University (TF).

References

- [1] D. Wulich and L. Goldfeld, "Bound of the distribution of instantaneous power in single carrier modulation," *IEEE Trans. Wireless Commun.*, **4**, 4, July 2005, pp. 1773–1778, doi:10.1109/TWC.2005.850309.
- [2] M. Tanahashi and H. Ochiai, "Analysis and efficient computation of instantaneous power distribution of single-carrier signals," in *GLOBECOM 2009 - 2009 IEEE Global Telecommun. Conf.*, November 2009, pp. 1–6, doi:10.1109/GLOCOM.2009.5425666.
- [3] —, "On the distribution of instantaneous power in single-carrier signals," *IEEE Trans. Wireless Commun.*, **9**, 3, March 2010, pp. 1207–1215, doi:10.1109/TWC.2010.03.091023.

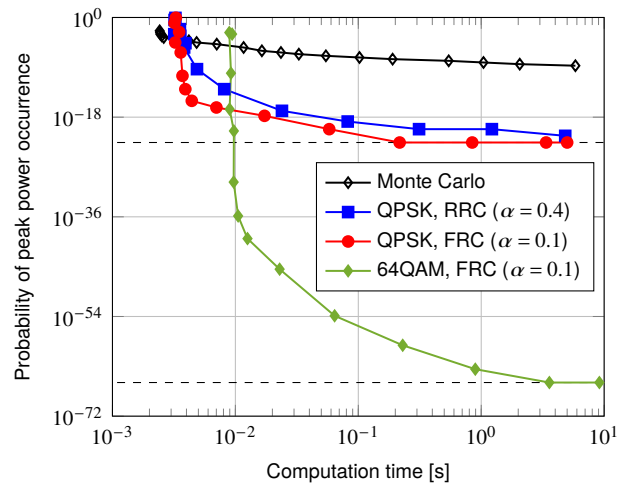


Figure 3. Comparison of obtained probabilities of peak power occurrence with respect to computation time. The dashed lines indicate the theoretical values.

- [4] H. Ochiai, "Exact and approximate distributions of instantaneous power for pulse-shaped single-carrier signals," *IEEE Trans. Wireless Commun.*, **10**, 2, December 2011, pp. 682–692, doi:10.1109/TWC.2011.120810.100755.
- [5] I. Gutman and D. Wulich, "Distribution of instantaneous power in single carrier signal with independent I/Q components," *IEEE Trans. Wireless Commun.*, **11**, 10, August 2012, pp. 3660–3667, doi:10.1109/TWC.2012.081312.112101.
- [6] European Telecommunications Standards Institute, "Second generation framing structure, channel coding and modulation systems for Broadcasting, Interactive Services, News Gathering and other broadband satellite applications; Part 1 (DVB-S2)," ETSI EN 302 307-1 (V1.4.1), November 2014.
- [7] Consultative Committee for Space Data Systems, "Flexible Advanced Coding and Modulation Scheme for High Rate Telemetry Applications," CCSDS 131.2-B-1, March 2012.
- [8] Y. Suzuki and H. Sujikai, "Transmission system of 4K/8K UHDTV satellite broadcasting," *IEICE Trans. Commun.*, **E103-B**, 10, October 2020, pp. 1050–1058, doi:10.1587/transcom.2019CBI0001.
- [9] T. Fukami, H. Saito, and A. Hirose, "Recursive Probability Mass Function Method to Calculate Probability Distributions of Pulse-Shaped Signals," *IEICE Trans. Fundamentals*, submitted.
- [10] W. H. Tranter, K. Sam Shanmugan, T. S. Rappaport, and K. L. Kosbar, *Principles of Communication Systems Simulation with Wireless Applications*, 1st ed. USA: Prentice Hall Press, December 2003.